Reaction of C_{60} with oxygen adatoms on Pt(111)

Cite as: J. Chem. Phys. **110**, 1173 (1999); https://doi.org/10.1063/1.478187
Submitted: 10 July 1998 . Accepted: 19 August 1998 . Published Online: 24 December 1998

Hong He, Nathan Swami, and Bruce E. Koel

Reaction of C_{60} with oxygen adatoms on Pt(111)

Hong He, Nathan Swami, and Bruce E. Koel
Departments of Chemistry and Materials Science, University of Southern California, Los Angeles, California 90088-0482

(Received 10 July 1998; accepted 19 August 1998)

Reactions of a C_{60} monolayer with oxygen adatoms on the Pt(111) surface were studied by a multitechnique surface science approach in the 100–1100 K range. Temperature programmed desorption (TPD), x-ray photoelectron spectroscopy (XPS), ultraviolet (UV) photoelectron spectroscopy (UPS), and high resolution electron energy loss spectroscopy (HREELS) were used to determine the onset temperature for the initial reaction and to characterize the reaction intermediates and products. Unlike the reaction of C_{60} with $O_{2(g)}$, which begins at 370 K, reaction with oxygen adatoms on Pt(111) begins below 100 K with the formation of C=O bonds with ν(CO) at 2134 cm^{-1}. At about 450, R–O–R species, where R=sp^2-hybridized carbon atoms singly bonded to oxygen, with ν(CO)=1215 cm^{-1}, develop and become the dominant reaction intermediates at 700–800 K. Also at these temperatures, an intense peak develops in the HREELS spectra characteristic of polymerized C_{60} at 1460 cm^{-1}. The reaction products decompose to liberate gas phase CO and CO_2 and form graphitic carbon. A prominent difference between the intermediates of this reaction and that of C_{60} with $O_{2(g)}$ is the absence of vibrational peaks in the 1650–1750 cm^{-1} region that arise from carbonyl groups. An R–O–R intermediate derived from the opening of pentagons in C_{60}, a structure that has not been observed experimentally before but has been suggested to be stable from theoretical calculations, is most consistent with our spectroscopic results. © *1999 American Institute of Physics.* [S0021-9606(98)70144-8]

I. INTRODUCTION

The oxidation of C_{60}, although not as facile as the reduction of fullerenes, has been carried out by a variety of methods.[1–10] Initial studies[1,2] focused on thermal oxidation of C_{60} films in an oxygen environment, while later studies reported phototransformations of C_{60} in benzene solution to $C_{60}O$[3] and $C_{60}O_2$,[4] and light-induced scission of C_{60} thin films by oxygen.[5] The chemical oxidation of C_{60} by XeF_2[6] or by reaction with superacid to form the C_{60}^+ cation[7] has also been reported. The electrochemical oxidation of C_{60} films[8] and solutions[9] has also been carried out at comparatively high anodic potentials. More recently, the oxidation of C_{60} films was performed using ozone.[10–12] Studies of the mechanism of reaction of C_{60} films with $O_{2(g)}$ by calorimetric[1,13] and spectroscopic methods[14–17] have determined that thermally induced oxidation starts at 370 K, with cage opening at 470 K and complete degradation of the fullerenes by 570 K.

Until now, no study of C_{60} oxidation by oxygen adatoms on metal surfaces has been published. Recent studies of the oxidation of C_{60} with ozone suggest that ozone oxidation is five orders of magnitude greater than that by $O_{2(g)}$[11] and the reaction generates odd-numbered carbon clusters that could provide a new route to functionalization and derivatization of fullerenes. In this respect, studies of the reaction of C_{60} with oxygen adatoms would be useful in delineating the differences between C_{60} oxidation by O_2, O_3, and O adatoms. Oxygen is dissociatively adsorbed on Pt(111) at room temperature to form oxygen adatoms, with a maximum surface coverage of 0.25 ML.[18,19] In this paper the reaction of monolayer C_{60} with oxygen adatoms on the Pt(111) surface is studied by using primarily x-ray photoelectron spectroscopy (XPS), UV-photoelectron spectroscopy (UPS), high resolution electron energy loss spectroscopy (HREELS), and temperature programmed desorption (TPD) to determine the temperature for the onset of oxidation and to characterize some of the reaction intermediates and products.

II. EXPERIMENT METHODS

The experiments were conducted in a three-level ultrahigh-vacuum chamber with a base pressure of 2×10^{-10} Torr, as has been described previously.[20] The top level was equipped with a double-pass cylindrical mirror analyzer (CMA) that was used for Auger electron spectroscopy (AES), XPS, and UPS. The middle level was equipped with low energy electron diffraction (LEED) optics and a quadrupole mass spectrometer (QMS) for TPD studies. The bottom level contained an LK2000 spectrometer for HREELS. The Pt(111) crystal was mounted on two Ta rods that were fastened to liquid-nitrogen cooled copper blocks at the bottom of a differentially pumped XYZ manipulator. The sample could be cooled to 90 or resistively heated to 1200 K. The Pt(111) sample was cleaned by a standard combination of Ar^+ ion sputtering at 5×10^{-5} Torr, annealing at 800 K in 5×10^{-8} Torr O_2 and flashing to 1200 K in vacuum. Sample cleanliness was checked with AES, LEED, and HREELS.

Oxygen adatoms were formed by dissociative adsorption of O_2 on the Pt(111) surface at 300 K. LEED was used to confirm the (2×2) overlayer structure at $\theta_o=0.25$ ML and the relative oxygen coverages were calibrated by O_2 TPD studies. C_{60} (99.9% purity, MER Corp.) was deposited on the

clean or oxygen-precovered Pt(111) surface at 100 K. The absence of substantial hydrocarbon impurities from C_{60} deposition was confirmed by the absence of any detectable C–H stretching mode in HREELS.

TPD studies utilized a temperature ramp of 4 K/s and a line-of-sight QMS arrangement. XPS spectra were obtained using Mg Kα photons (1253.6 eV) to excite the core levels and obtain spectra at an analyzer resolution of 400 meV. All binding energies were referenced to that of the Pt($4f_{7/2}$) level at 71.2 eV.[21] He(*I*) (21.2 eV) UPS spectra were obtained using a high pressure discharge lamp and spectra were acquired at an analyzer resolution of 300 meV. The HREELS spectra were recorded in the specular scattering direction with an angle of 60 deg from the surface normal and an incident electron beam energy of 4.5 eV. The overall energy resolution of the spectrometer was less than 6 meV (50 cm^{-1}), and the count rates at the elastic peak were about 100 kHz for clean Pt(111). The spectra reported were normalized to the intensity of the elastic peak. AES studies of the deposition of C_{60} on Pt(111) at 100 K were used to determine the monolayer formation conditions, and we assigned monolayer coverage to the first ''break point'' in the uptake curve.[20]

III. RESULTS

A. Temperature programmed desorption (TPD) studies

TPD provides us with a quick method to check for thermal reactions between C_{60} and oxygen adatoms in the 100–1000 K temperature range and to identify the reaction products that desorb from the surface. The masses monitored include 2 (H_2), 12 (C), 16 (O), 18 (H_2O) 28 (CO), 32 (O_2), and 44 amu (CO_2). The reaction products from C_{60} oxidation desorbed from the surface mainly as CO and CO_2. Figure 1 shows the results for desorption of CO, CO_2, and O_2 for the 1 ML C_{60}/O(2×2)/Pt(111) system in the 100–1000 K temperature range. Control experiments studying desorption from O(2×2)/Pt(111) and 1 ML C_{60}/Pt(111) surface are also shown. Oxygen desorbs from the O(2×2)/Pt(111) surface at 758 K and the area under the O_2 TPD peak was defined as $\theta_o = 0.25$ ML. The lower portion of Fig. 1 shows that all of the surface oxygen was reacted with C_{60}, and no O_2 desorption occurred for 1 ML C_{60}/O(2×2)/Pt(111). Three peaks were seen for CO_2 at 325, 410, and 510 K. The CO_2 peaks at 325 and 410 K were due primarily to desorption from oxidation of coadsorbed CO from the background as judged by the CO_2 peaks in the TPD for O(2×2)/Pt(111). The CO_2 peak at 510 K was absent in both of the control studies and so it arises from the reaction of C_{60} with oxygen adatoms. The CO TPD spectra showed four main peaks at 325, 510, 570, and 945 K. The peaks at 325 and 510 K were probably due to cracking of the CO_2 product. The CO TPD peak from contaminant coadsorbed CO for a C_{60} monolayer on Pt(111) was at 460 K. Thus the development of the two peaks at 570 and 945 K was entirely due to reaction products from C_{60} oxidation reactions. The total amount of CO obtained from the oxidation of C_{60} at these conditions was about 0.07 ML CO by reference to the saturation CO coverage of $\theta_{CO} = 0.68$ ML on Pt(111) at 100 K.[22] The total amount of CO_2 obtained was estimated to be about 0.09 ML by mass balance. The CO_2 peaks at 325 and 510 K, and the CO peaks at 570 and 945 K were used to determine annealing temperatures for the subsequent spectroscopic studies.

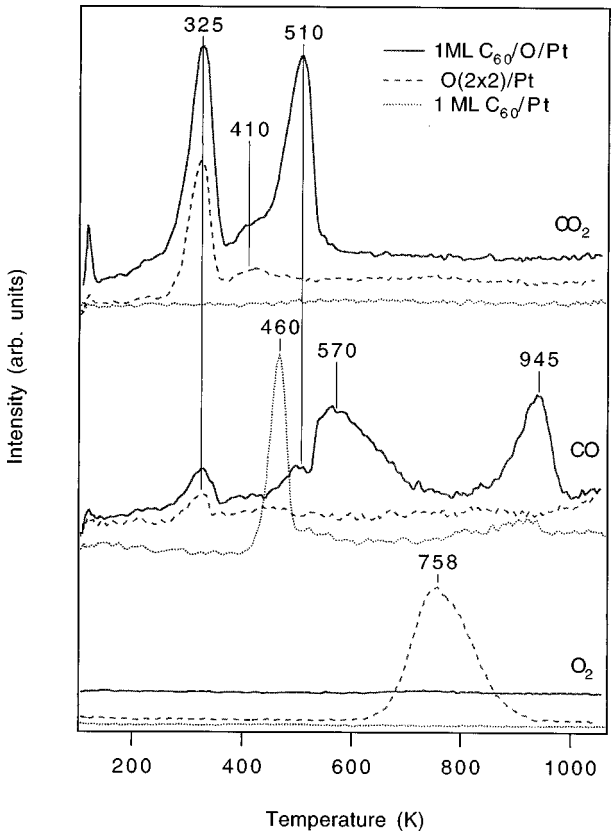

FIG. 1. TPD spectra obtained from 1 ML C_{60}/O(2×2)/Pt(111) (_____), O(2×2)/Pt(111) (----), and 1 ML C_{60}/Pt(111) (.....) .

B. UPS studies

UPS studies were conducted to determine the onset temperature for the reaction of C_{60} with oxygen adatoms on Pt(111). However, since previous researchers have suggested that C_{60} reacts with Pt,[23,24] the chemisorption of C_{60} on Pt(111) in the absence of surface oxygen was studied by UPS to better characterize this chemistry. Figure 2 shows UPS spectra for the C_{60} monolayer on Pt(111) after heating to different substrate temperatures. The C_{60} multilayer (~10 ML) spectrum shows clearly the distinctive five band structure of solid C_{60}.[25] The C_{60} monolayer deposited on Pt(111) at 100 K also shows these distinctive features but several of the peaks are shifted toward the Fermi level in comparison to solid C_{60}. Since such shifts are expected for chemisorbed species, we believe that the C_{60} monolayer on Pt(111) at 100 K is most likely to be molecularly chemisorbed. A more extensive study published elsewhere[20] presents evidence that points to polymerization of submonolayer amounts of C_{60} catalyzed by Pt(111) at 300 K and decomposition of C_{60} at temperatures of 700 K and higher. The UPS spectra obtained after heating to 700 and 1100 K thus characterize decomposed C_{60}. The UPS spectra for the C_{60} monolayer deposited

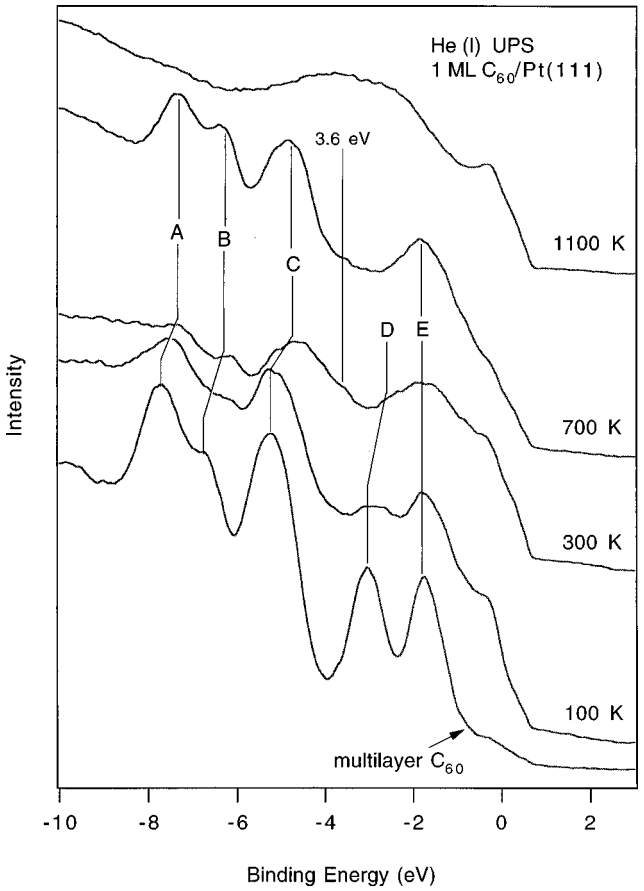

FIG. 2. UPS spectra showing the shifts of the five band structure of C_{60} toward the Fermi energy for temperatures of 300 K or higher. The spectra at 100 and 300 K were acquired by 1 ML C_{60} deposition at these temperatures, and the spectra at 700 and 1100 K were taken by annealing C_{60} multilayers. The UPS spectrum of solid C_{60} is also shown, as obtained by depositing 4 ML C_{60} on Pt(111) at 100 K.

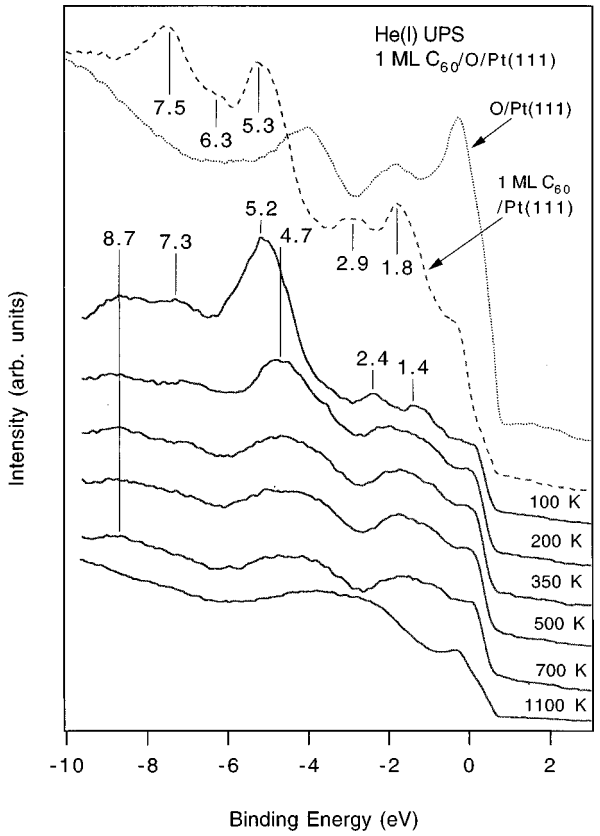

FIG. 3. UPS spectra after deposition of 1 ML C_{60} on O(2×2)/Pt(111) at 100 K and then annealing to higher temperatures. For comparison, we also show the UPS spectra of the O(2×2)/Pt(111) surface (....) and 1 ML C_{60}/Pt(111) at 100 K (--).

at 300 K show very weak features for the five band structure of C_{60} and more closely resemble the spectrum at 700 K than that at 100 K. This indicates decomposition on the Pt(111) surface at 300 K, as has been suggested in earlier reports.[23,24] For the spectra at 300 and 700 K substrate temperatures, a weak feature was seen near 3.6 eV similar to that of polymerized C_{60}.[26]

The reaction of C_{60} with oxygen adatoms was studied by forming the (2×2) oxygen adlayer ($\theta_o = 0.25$ ML) on Pt(111) at 300 K and then depositing 1 ML C_{60} on this surface at 100 K. The UPS ''warm-up'' spectra are shown in Fig. 3. The UPS spectra for 1 ML C_{60}/Pt(111) at 100 K and the O(2×2)/Pt(111) surface at 300 K are also included for comparison. Even at 100 K, the higher binding energy structures in the C_{60} valence band at 7.5 and 6.3 eV are absent for 1 ML C_{60}/O(2×2)/Pt(111). The lower binding energy structures of C_{60} have diminished intensities and are shifted to lower binding energies, consistent with alteration of the electronic structure of the molecule. A new broad feature is seen at about 8.7 eV and a new intense peak appears at 5.2 eV. Similar peaks appeared in UPS spectra of photoexcited C_{60} films on solid $O_{2(g)}$ at 20 K that were assigned to CO and CO_2[27] and that also correspond to peaks in carbonyl-type compounds.[28,29] After the 200 K anneal, C_{60} features were no longer apparent. The peak at about 5 eV is now the only discernible peak in the spectrum. Over the range of annealing temperatures of 350–700 K, the spectra are essentially unchanged, even though CO and CO_2 desorption occurs. Amorphous carbon features dominate the spectra, as characterized by weak π emission and the persistence of a dominant σ-π feature at about 5 eV.[30] Heating to 1100 K forms graphite. These results suggest that C_{60} reacts with oxygen adatoms on Pt(111) at temperatures below 100 K, producing eventually gas phase CO and CO_2, amorphous carbon, and graphite.

C. X-ray photoelectron spectroscopy (XPS) studies

The onset of oxidation reactions and the formation of intermediates can be probed by XPS studies of the O(1*s*) core level. XPS warm-up spectra for the 1 ML C_{60}/O(2×2)/Pt(111) system are shown in Fig. 4, along with those of O(2×2)/Pt(111) and 1 ML C_{60}/Pt(111) for comparison. The peak positions were determined by subtracting a background curve (dashed lines) from the experimental data points and then fitting Gaussian peaks of 1.5 eV full width at half maximum (FWHM) to obtain minimum residuals. The O(1*s*) peak for oxygen adatoms occurs at 529.4 eV BE (the small peak at 532 eV in the bottom curve is due to dissociation of water from the background). For 1 ML C_{60}/Pt/(111), the O(1*s*) spectrum is featureless, and hence the effect of background adsorption of water on the XPS warm-up spectra

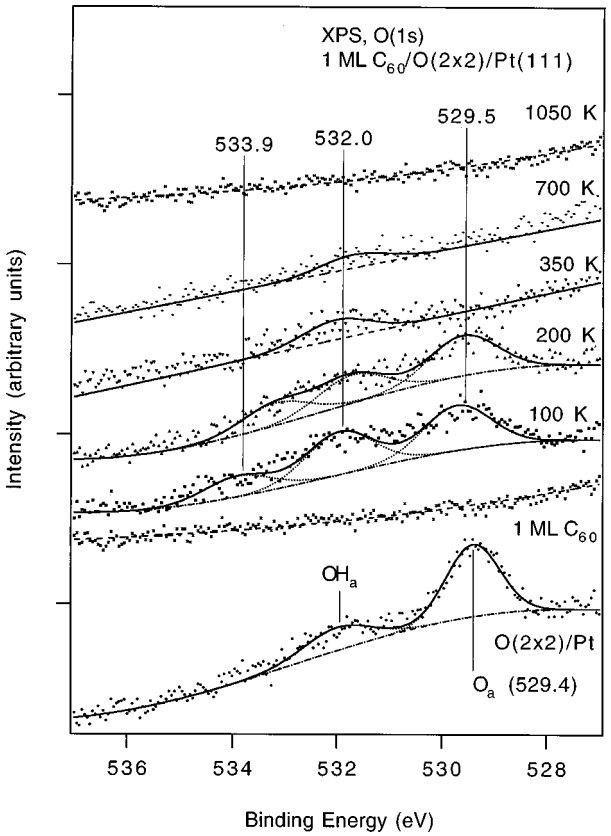

FIG. 4. O(1*s*) XPS spectra after deposition of 1 ML C_{60} on O(2×2)/Pt(111) at 100 K and then annealing to higher temperatures. For comparison, we also show the O(1*s*) XPS spectra for the O(2×2)/Pt(111) surface and 1 ML C_{60}/Pt(111) at 100 K.

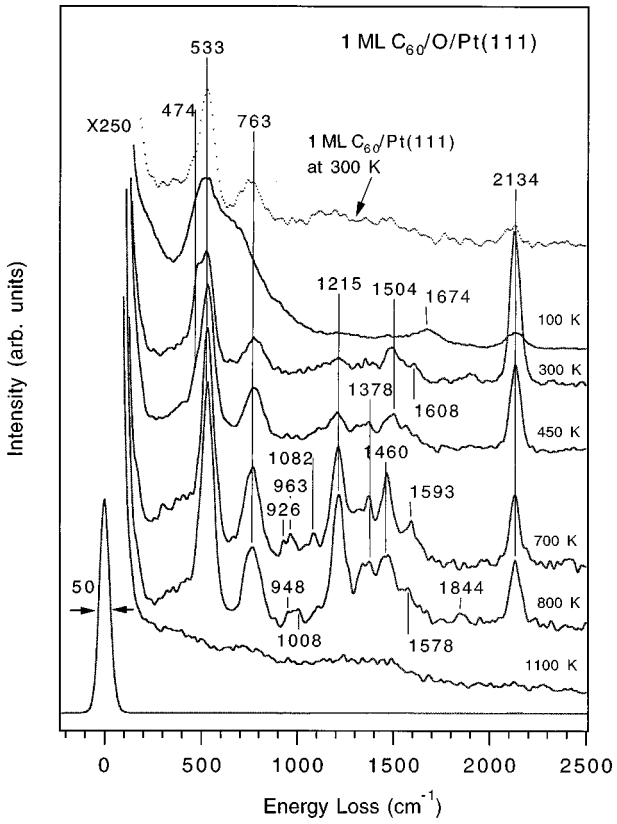

FIG. 5. HREELS spectra for 1 ML C_{60}/O(2×2)/Pt(111) at 100 K and following heating to higher temperatures. The spectrum for the 1 ML C_{60}/Pt(111) at 300 K is also shown as the top curve for comparison.

in Fig. 4 is minimal. After the adsorption of 1 ML C_{60} on the oxygen precovered surface at 100 K, the O(1*s*) peaks at 533.9 and 532.0 eV BE corresponding to reacted oxygen grow in at the expense of the oxygen adatom peak at 529.4 eV BE. The oxygen adatom peak persists until at least 200, but it is no longer present at 350 K. This evidence confirms that the reaction of C_{60} with oxygen adatoms begins at least by 100 and that all oxygen adatoms have reacted by 350 K.

The chemical shift in the O(1*s*) level between $O_{2(g)}$ and the molecules $CO_{(g)}$ and $CO_{2(g)}$ is 1.0 and 2.25 eV,[31] respectively, and that between $O_{2(g)}$ and oxygen in R–O–R and carbonyl (C=O) functional groups is 5.1 and 5.7 eV, respectively.[32] Using these chemical shifts referenced to the O(1*s*) level of $O_2(s)$ at 537 eV BE,[28] we estimate O(1*s*) BEs of condensed phase CO and CO_2 at 534 and 535 eV BE, respectively, and R–O–R and carbonyl (C=O) functional groups to have O(1*s*) levels at 531.3–531.9 eV BE. The large emission at 532 eV for the XPS spectra in Fig. 4 is assigned to R–O–R and/or carbonyl functional groups. The peak at 534 eV BE is assigned to CO. This peak shifts to about 0.5 eV lower BE after heating to 200 K, and disappears during the 350 K anneal, concomitant with the disappearance of the $O_{(a)}$ peak. This correlation will be important in our later discussion of the source of $CO_{2(g)}$ in TPD. Hence, these XPS results show that R–O–R and/or carbonyl functional groups are formed as reaction intermediates and they persist until high temperatures where further thermal decomposition leads to the formation and desorption from the surface of CO and CO_2.

D. High resolution electron energy loss spectroscopy (HREELS) studies

Vibrational spectra from HREELS also were used to determine the onset temperature for the oxidation reaction and to characterize the reaction products as the surface is heated. These warm-up spectra are shown in Fig. 5. As a reference, the top (dashed) curve in Fig. 5 reproduces the spectrum for 1 ML C_{60}/Pt(111) at 300 K. In this case, the main C_{60} features are the dipole active $T_{1u}(1)$, $T_{1u}(3)$, and dipole inactive $H_g(4)$ modes at 533, 1215, and 763 cm^{-1}. Depositing C_{60} on the oxygen precovered surface, i.e., O(2×2)/Pt(111), at 100 K gives rise to the top solid curve in Fig. 5. The Pt–O stretching mode appears at 474 cm^{-1}, and the C_{60} features resemble closely those found for 1 ML C_{60}/Pt(111) at 100 K. One striking feature for C_{60}/O(2×2)/Pt(111) at 100 K is the appearance of a mode at 2134 cm^{-1}. This peak increases in intensity after heating to 300 K, and persists on the surface with a reduced intensity until very high temperatures (T >800 K). The frequency of this peak is closer to the value of ν(CO) for gas phase CO at 2143 cm^{-1} [33] than the ν(CO) values for adsorbed CO on Pt(111) at 1950 cm^{-1} for bridge sites and 2060 cm^{-1} for atop sites.[22] This suggests that the CO giving rise to this loss peak is not bonded to Pt(111). This is consistent with the presence of this peak at the same frequency beyond the desorption temperature (460 K) for

CO TPD from C_{60}/Pt(111) as seen in Fig. 1 (dotted line). The nature of this CO species will be discussed further in Sec. IV.

Oxygen adatoms are still present on the surface at 300 K, giving rise to a peak at 474 cm^{-1}, but disappear by 450 K. This temperature is much below the O_2 desorption temperature of 758 K on clean Pt(111) as seen in Fig. 1.

Another striking feature in Fig. 5 is the ''rich'' nature of these warm-up spectra in the range 800–1600 cm^{-1}, with more high intensity peaks than were seen for 1 ML C_{60}/Pt(111), particularly for substrate temperatures greater than 300 K.[21] This shows that the icosahedral symmetry of C_{60} is lowered more extensively in the reactions with oxygen adatoms than with the clean Pt(111) surface. After heating to 700 K, large peaks are seen at 1215 and 1460 cm^{-1}. The dipole active $T_{1u}(4)$ mode of C_{60}, which usually appears at 1430 cm^{-1}, is dwarfed by the high intensity Raman active $A_g(2)$ mode at 1460 cm^{-1} that has been assigned by Duclos *et al.*[15,16] to arise from the incorporation of oxygen into C_{60} films. We believe that the mode developing at 1460 cm^{-1} does not arise from the $T_{1u}(4)$ mode since it does not obey the expected ratio for the relative intensities of the modes $T_{1u}(1):T_{1u}(2):T_{1u}(3):T_{1u}(4)=100:29:6:5$.[34] The appearance of a prominent mode at 1460 cm^{-1} in the infrared (IR) spectrum has been identified with polymerization of C_{60}.[35,36]

In previous, related IR studies of the reaction of C_{60} films with $O_{2(g)}$, modes at 700–1100 cm^{-1} were assigned to epoxide species[17,37] and modes at 1500–1600 cm^{-1} were assigned to C=C stretches for aromatic and olefinic species,[17,37] modes at 1000 and 1080 cm^{-1} were assigned to $C_{60}O_2$,[35] and a mode at 1237 cm^{-1} was assigned to sp^2 hybridized carbon singly bonded to oxygen.[38,39] In our spectra shown in Fig. 5, we assign peaks at 920–1080 cm^{-1} to epoxide species, the peak at 1215 cm^{-1} to sp^2 hybridized carbon singly bonded to oxygen,[37] and the peak at 1460 cm^{-1} to polymerization of C_{60}. A notable difference between our results and those for C_{60} films reacting with gas phase O_2 is the absence of peaks in our spectra at 1600–1800 cm^{-1} that were assigned to carbonyl (C=O) groups[14,17] and 2320 cm^{-1} that were assigned to CO_2.[17]

IV. DISCUSSION

C_{60} readily reacts with oxygen adatoms on Pt(111). Indeed the onset temperature for reaction is less than 100 K, and we can roughly estimate an activation barrier for initiation of this reaction that is less than 8 kcal/mol. While the HREELS spectra and structure of C_{60} are not altered greatly on Pt(111) until graphization at 1050 K,[21] significant changes occur in the vibrational spectra of 1 ML C_{60}/O(2×2)/Pt(111) due to intermediates formed by reaction of C_{60} with oxygen adatoms. The reaction products ultimately formed upon heating the surface were $CO_{(g)}$, $CO_{2(g)}$, and amorphous and graphitic carbon. Reaction intermediates include polymerized C_{60}, R–O–R functional groups containing sp^2 hybridized carbon species singly bonded in oxygen, and to a smaller extent epoxide species and aromatic and olefinic species.

In previous studies of the oxidation of C_{60} films with $O_{2(g)}$,[17] intercalation of the CO(*g*) product was observed. This is consistent with intercalation of the C_{60} lattice with O_2 at low temperatures (<300 K) in the range of 75–375 Torr $O_{2(g)}$, prior to the onset of reaction with C_{60} at 370 K.[17,40] CO in our studies begins to form at low temperatures (100–300 K) and it is possible that this product is present either inside the modified C_{60} cage or intercalated between the Pt surface and the C_{60} adlayer (but not in a geometry suitable for CO chemisorption). The CO stretching frequency in Fig. 5 at 2134 is between that of 2127 cm^{-1} for CO intercalated in a C_{60} lattice[41] and 2143 cm^{-1} for free CO gas,[32] and hence CO could be inside the modified C_{60} cage. This CO could be responsible for the high temperature TPD peak at 945 K. The other desorption peak for CO at 570 K is probably due to a different source such as decomposition of the C_xO_y intermediate(s) whose structure will be discussed later,

$$C_xO_{y(a)} \overset{570\ K}{\rightarrow} C_{x-1}O_{y-1(a)} + CO_{(g)}. \quad (1)$$

The CO_2 product does not come from reactions of carbonyl groups. No carbonyl functional groups were observed in HREELS, i.e., no peaks occurred in the 1650–1750 cm^{-1} region in Fig. 5. We propose that unreacted oxygen adatoms still present on the surface at 300 K are responsible for the oxidation of the C_xO_y species and CO formed at lower temperatures to produce CO_2 as follows:

$$C_xO_{y(a)} + O_{(a)} \overset{325-510}{\rightarrow} CO_{2(g)} + C_{x-1}O_{y-1(a)},$$

$$CO_{(a)} + O_{(a)} \overset{325-510}{\rightarrow} CO_{2(g)}.$$

A proposal for the sequence of steps as the temperature of the surface is gradually raised from 100 to 1000 K is as follows. Oxygen adatoms break some bonds of C_{60} to form C_xO_y species and some CO that is intercalated or trapped inside of the modified cage. The reactive C_xO_y species and CO react with oxygen adatoms forming $CO_{2(g)}$ in the 300–500 K temperature range. At about 450 K, bonds of the R–O–R type develop and such species become the dominant reaction intermediates at 700–800 K. Concomitant to R–O–R formation, polymerization of C_{60} and formation of aromatic and olefinic species occurs. These reactions reduce the icosahedral symmetry of the molecule and heating to 700 K may result in cage opening. The final step is the formation of amorphous carbon and graphite with the release of all oxygen from the adlayer in the form of CO and CO_2.

Figure 6(a) shows a region in the C_{60} molecule comprised of pentagons and sp^2 hybridized hexagons where initial reaction with oxygen could occur. Figures 6(b)–6(d) show several possible structures for reaction intermediates based on our HREELS assignments and previous work.[3,42–44] Strain relief was suggested to be a major driving force for the reactions of C_{60}.[45] The epoxide in Fig. 6(b) formed by attacking one of the double bonds[3,42] is unstable because it presents a high local strain on the globally strained C_{60} molecule,[45] and so subsequent reaction could form either of the two R–O–R species, (where R is sp^2 hybridized carbon) shown in Figs. 6(c) and 6(d). On the other hand, it is possible that oxygen adatoms may attack the pentagon–pentagon single bond to directly form the structure in Fig. 6(d), since

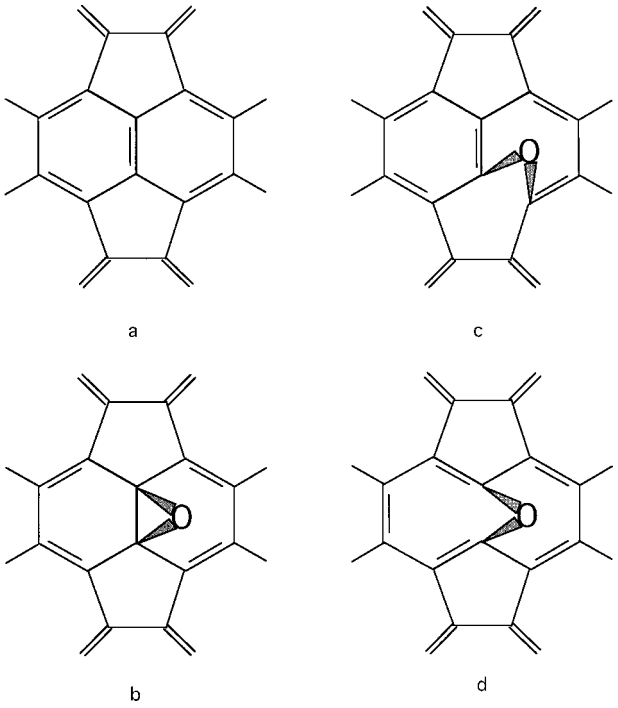

FIG. 6. Schematic drawings of C_{60} and several possible structures for C_{60} oxidation intermediates based on HREELS: (a) pristine C_{60}; (b) epoxide intermediate; and two possibilities (c) and (d) for R–O–R intermediates, where R is sp^2 hybridized carbon.

fullerenes favor reactions that decrease strain.[45] The hexagon–O–pentagon structure in Fig. 6(c) was proposed to be more stable than the hexagon–O–hexagon structure in Fig. 6(d) from theoretical studies,[43] but has so far not been observed experimentally.[44] The structure in Fig. 6(d) has been argued to be unlikely in a recent study[44] since it placed double bonds in two pentagons. In our HREELS results, the intensity of the peaks in the 900–1100 cm^{-1} region for the epoxide species is far lower than that of the peak at 1215 cm^{-1} corresponding to the R–O–R species. Hence, we believe that the structure in Fig. 6(c) is an important intermediate. This represents the first experimental observation of this species. We note that if all of the 12 pentagons of C_{60} were opened up in the manner shown in Fig. 6(c), then this structure is consistent with observations that the maximum oxygen uptake of pure C_{60} occurs at $O/C_{60}=12$.[1,39] Finally, we note that an ''on top'' isomer suggested by theoretical calculations[43] is not shown in Fig. 6 because we observed no carbonyl bands for the intermediates. However, linked species like the $C_{120}O$ dimer[46] are consistent with our results identifying polymerization and R–O–R linkages, and certainly are possible intermediates.

The oxidation of C_{60} in our studies is initiated by oxygen atoms on the O/Pt(111) surface, and the oxidation differs considerably from that with $O_{2(g)}$ (in the absence of any catalyst), where O_2^- ions may be the reactive species,[25,28] in the following ways:

(1) The onset temperature for oxidation reactions by O/Pt(111) is less than 100 K, while it is 370 K for $O_{2(g)}$.[17] For oxidation with $O_{2(g)}$, cage opening starts at 470 and is complete by 570 K, as determined by the spectroscopic identification of amorphous carbon.[17] For the case of oxidation with O adatoms on Pt(111), cage opening and complete fragmentation does not occur until much higher temperatures ($T>700$–950 K); however, this chemistry is likely dominated by C_{60}/Pt(111) interactions given the low stoichiometry of oxygen present.
(2) Unlike in oxidation with $O_{2(g)}$, carbonyl species were not detected as stable intermediates for oxidation with O/Pt(111).
(3) The reaction of C_{60} with oxygen adatoms on Pt(111) apparently promotes polymerization of C_{60} compared to that for $O_{2(g)}$. However, in the initial stages of interaction of C_{60} with $O_{2(g)}$, intercalation of the C_{60} lattice occurs which suppresses polymerization.[47]
(4) For C_{60} oxidation with $O_{2(g)}$, ν(CO) was seen at 2127 cm^{-1},[14] exactly at the value for CO intercalated into C_{60},[41] while for C_{60}/O/Pt(111) it occurs at 2134 cm^{-1}, very close to the gas phase value, and hence it is possible that CO could present inside the modified C_{60} cage.

The oxidation of C_{60} with O adatoms on Pt(111) bears a close resemblance to that with $O_{3(g)}$ (in the absence of catalyst). In both of these cases, the oxidation process is more facile than with $O_{2(g)}$ and begins at lower temperatures.[11] Further, in both cases polymerization of C_{60} is promoted by the oxidation process.[10–13]

C_{60} oxidation using $O_{3(g)}$ leads to many odd-numbered carbon clusters such as C_{119}, and this was suggested to represent a new route to functionalization and derivatization of fullerenes.[10] The intermediates formed by the oxidation of C_{60} with O adatoms on metal surfaces could have the same potential. Further work is needed to realize this potential use of catalyzed surface oxidation reactions.

V. CONCLUSIONS

The oxidation of a C_{60} monolayer by oxygen adatoms on a Pt(111) surface is a facile reaction, much like that with $O_{3(g)}$ in the absence of any catalyst. The onset temperature for the surface reaction is less than 100 K. The reaction intermediates are polymerized C_{60}, R–O–R species with sp^2 hybridized carbon atoms singly bonded to oxygen, and to a smaller extent epoxide species and aromatic and olefinic species. The reaction intermediates decompose at high temperatures to produce the gas phase reaction products CO and CO_2, forming amorphous and eventually graphitic carbon. Using vibrational spectroscopy we identify a particular R–O–R intermediate formed by the opening of pentagons in C_{60}, and this represents the first experimental observation of this structure which has been suggested to be a stable intermediate in C_{60} oxidation from theoretical calculations.

ACKNOWLEDGMENTS

We acknowledge support of this work by the Divisions of Chemistry and Materials Research of the National Science Foundation. We also thank Dr. Robert Bolskar of USC for helpful discussions.

[1] H. S. Chen, A. R. Kortan, R. C. Haddon, M. L. Kaplan, C. H. Chen, A. M. Mujsce, H. Chou, and D. A. Fleming, Appl. Phys. Lett. **59**, 2956 (1991).

[2] J. Milliken, T. M. Keller, A. P. Baronavski, S. W. McElvany, J. H. Callahan, and H. H. Nelson, Chem. Mater. **3**, 386 (1991).
[3] K. M. Creegan, J. L. Robbins, W. K. Robbins, J. M. Millar, R. D. Sherwood, P. J. Tindall, D. M. Cox, A. B. Smith, III, J. P. McCauley, Jr., D. R. Jones, and R. T. Gallagher, J. Am. Chem. Soc. **114**, 1103 (1992).
[4] D. Heymann and L. P. F. Chibante, Chem. Phys. Lett. **207**, 339 (1993).
[5] C. Taliani, G. Ruani, R. Zamboni, R. Danieli, S. Rossini, V. N. Denisov, V. M. Burlakov, F. Negri, G. Orlandi, and F. Zerbetto, J. Chem. Soc. Chem. Commun. , 220 (1993).
[6] K. O. Christe and W. W. Wilson, Paper #66, presented at 203rd ACS meeting, San Francisco, 1992.
[7] G. P. Miller, C. S. Hsu, L. Y. Chieng, H. Thomann, and M. Bernado, Chem. Eng. News **69**, 17 (1991).
[8] C. Jehoult, A. J. Bard, and F. Wudl, J. Am. Chem. Soc. **113**, 5456 (1991).
[9] D. Dubios, K. M. Kadish, S. Flanagan, and L. J. Wilson, J. Am. Chem. Soc. **113**, 7773 (1991).
[10] S. W. McElvany, J. H. Callahan, M. M. Ross, L. D. Lamb, and D. R. Huffman, Science **260**, 1632 (1993).
[11] L. P. F. Chibante and D. Heymann, Geochim. Cosmochim. Acta **57**, 1879 (1993).
[12] J. P. Deng, C. Y. Mou, and C. C. Han, Fullerene Sci. Technol. **5**, 1033 (1997).
[13] H. S. Chen, A. R. Kortan, R. C. Haddon, and D. A. Fleming, J. Phys. Chem. **96**, 1016 (1992).
[14] H. Werner, Th. Schedel-Niedrig, M. Wohlers, D. Herein, B. Herzog, R. Schlögl, M. Keil, A. M. Bradshow, and J. Kirschner, J. Chem. Soc., Faraday Trans. **90**, 403 (1994).
[15] S. J. Duclos, R. C. Haddon, S. H. Glarum, A. F. Hebard, and K. B. Lyons, Solid State Commun. **80**, 481 (1991).
[16] S. J. Duclos, R. C. Haddon, S. Glarum, A. F. Hebard, and K. B. Lyons, Science **254**, 1625 (1991).
[17] M. Wohlers, H. Werner, D. Herein, T. Schedel-Niedrig, A. Bauer, and R. Schlögl, Synth. Met. **77**, 299 (1996).
[18] C. T. Campbell, G. Ertl, H. Kuipers, and J. Segner, Surf. Sci. **107**, 220 (1981).
[19] J. L. Gland, B. A. Sexton, and G. B. Fisher, Surf. Sci. **95**, 587 (1980).
[20] N. Swami, H. He, and B. E. Koel, Phys. Rev. B (in press).
[21] *Handbook of X-Ray Photoelectron Spectroscopy* (Perkin-Elmer Corporation, 1992).
[22] M. T. Paffett, S. C. Gebhard, R. G. Windham, and B. E. Koel, J. Phys. Chem. **94**, 6831 (1990).
[23] H. P. Lang, V. Thommen-Geiser, J. Frommer, A. Zahab, P. Bernier, and H.-J. Güntherodt, Europhys. Lett. **18**, 29 (1992).
[24] W. I. F. David, R. M. Ibberson, J. C. Matthewman, K. Prassides, F. J. S. Dennis, J. P. Hare, H. W. Kroto, R. Taylor, and D. R. M. Walton, Nature (London) **353**, 147 (1991).
[25] D. L. Liehtenberger, K. W. Nebesny, C. D. Ray, D. R. Huffman, and L. D. Lamb, Chem. Phys. Lett. **176**, 203 (1991).
[26] A. Ito, T. Morikawa, and T. Takahashi, Chem. Phys. Lett. **211**, 333 (1993).
[27] G. H. Kroll, P. J. Benning, Y. Chen, T. R. Ohno, J. H. Weaver, L. P. F. Chibante, and R. E. Smalley, Chem. Phys. Lett. **181**, 112 (1991).
[28] C. S. Fadley, in *Electron Spectroscopy: Theory, Techniques and Applications*, edited by C. R. Brundle and A. D. Baker (Academic, New York, 1978), p. 156.
[29] E. W. Plumer, W. R. Salaneck, and J. S. Miller, Phys. Rev. B **18**, 1673 (1978).
[30] A. Bianconi, S. M. B. Hagström, and R. Z. Bachrach, Phys. Rev. B **16**, 5443 (1977).
[31] K. Siegbahn, C. Nordling, G. Johansson, J. Hedman, P. F. Heden, K. Hamrin, V. Gelius, T. Bergmark, L. O. Werne, R. Manne, and Y. Baer, *ESCA Applied to Free Molecules* (North Holland, Amsterdam, 1969), p. 125.
[32] J. S. Jen and T. D. Thomas, J. Electron Spectrosc. Relat. Phenom. **4**, 43 (1974).
[33] K. Nakamoto, *Infrared Spectra of Inorganic and Coordination Compounds* (Wiley, New York, 1963), p. 72.
[34] G. Gensterblum, L.-M. Yu, J. J. Pireaux, P. A. Thiry, R. Caudano, P. Lambin, A. A. Lucas, W. Krätschmer, and J. E. Fischer, J. Phys. Chem. Solids **53**, 1427 (1992).
[35] A. M. Rao, K-A. Wang, J. M. Holden, Y. Wang, P. Zhou, P. C. Eklund, C. C. Eloi, and J. D. Robertson, J. Mater. Res. **8**, 2277 (1993).
[36] M. S. Dresselhaus, G. Dresselhaus, and P. C. Eklund, J. Mater. Res. **8**, 2054 (1993).
[37] *Atlas of Spectral Data and Physical Constants for Organic Compounds*, edited by J. G. Graselli and W. M. Ritchey, 2nd ed (CRC, Boca Raton, FL, 1975), Vol. I, p. 335.
[38] J. C. Scalon, J. M. Brown, and L. B. Ebert, J. Phys. Chem. **98**, 3921 (1994).
[39] J. A. Nisha, V. Sridharan, J. Janaki, Y. Hariharan, V. S. Sastry, C. S. Sundar, and T. S. Radhakrishnan, J. Phys. Chem. **100**, 4503 (1996).
[40] M. Wohlers, A. Bauer, T. Ruhle, F. Neitzel, H. Werner, and R. Schlogl, Fullerene Sci. Technol. **5**, 49 (1997).
[41] I. Holleman, G. von Helden, E. H. T. Olthof, P. J. M. van Bentum, R. Engein, G. H. Nachtegael, A. P. M. Kentgens, B. H. Meir, A. van der Avoird, and G. Meijer, Phys. Rev. Lett. **79**, 1138 (1997).
[42] A. Hirsch, *The Chemistry of Fullerene* (Geory Thierre Verlag, Stuttgart, 1994), p. 164.
[43] K. Raghavachari and C. Sosa, Chem. Phys. Lett. **209**, 223 (1993).
[44] V. N. Bezmelnitsin, A. V. Eletskii, N. G. Schepetov, A. G. Arent, and R. Taylor, J. Chem. Soc., Perkin Trans. **2**, 683 (1997).
[45] R. C. Haddon, Science **261**, 1545 (1993).
[46] S. Lebedkin, S. Ballenweg, J. Gross, R. Taylor, and W. Krätschmer, Tetrahedron Lett. **36**, 4971 (1995).
[47] P. Zhou, A. M. Rao, K.-A. Wang, J. D. Robertson, C. Eloi, M. S. Meier, S. L. Ren, X.-X. Bi, P. C. Eklund, and M. S. Dresselhaus, Appl. Phys. Lett. **60**, 2871 (1992).